

Solution of the Schrödinger equation by a spectral method II: Vibrational energy levels of triatomic molecules@fa@f)

M. D. Feit and J. A. Fleck

Citation: *J. Chem. Phys.* **78**, 301 (1983); doi: 10.1063/1.444501

View online: <http://dx.doi.org/10.1063/1.444501>

View Table of Contents: <http://jcp.aip.org/resource/1/JCPSA6/v78/i1>

Published by the [American Institute of Physics](#).

Additional information on J. Chem. Phys.

Journal Homepage: <http://jcp.aip.org/>

Journal Information: http://jcp.aip.org/about/about_the_journal

Top downloads: http://jcp.aip.org/features/most_downloaded

Information for Authors: <http://jcp.aip.org/authors>

ADVERTISEMENT



Goodfellow
metals • ceramics • polymers • composites
70,000 products
450 different materials
small quantities *fast*

www.goodfellowusa.com

Solution of the Schrödinger equation by a spectral method

II: Vibrational energy levels of triatomic molecules^{a)}

M. D. Feit and J. A. Fleck, Jr.

University of California, Lawrence Livermore National Laboratory, Livermore, California 94550
(Received 16 August 1982; accepted 27 September 1982)

The spectral method utilizes numerical solutions to the time-dependent Schrödinger equation to generate the energy eigenvalues and eigenfunctions of the time-independent Schrödinger equation. Accurate time-dependent wave functions $\psi(\mathbf{r}, t)$ are generated by the split operator FFT method, and the correlation function $\langle \psi(\mathbf{r}, 0) | \psi(\mathbf{r}, t) \rangle$ is computed by numerical integration. Fourier analysis of this correlation function reveals a set of resonant peaks that correspond to the stationary states of the system. Analysis of the location of these peaks reveals the eigenvalues with high accuracy. Additional Fourier transforms of $\psi(\mathbf{r}, t)$ with respect to time generate the eigenfunctions. Previous applications of the method were to two-dimensional potentials. In this paper energy eigenvalues and wave functions obtained with the spectral method are presented for vibrational states of three-dimensional Born-Oppenheimer potentials applicable to SO_2 , O_3 , and H_2O . The energy eigenvalues are compared with results obtained with the variational method. It is concluded that the spectral method is an accurate tool for treating a variety of practical three-dimensional potentials.

I. INTRODUCTION

In a previous paper¹ we described a method for computing the eigenvalues and eigenfunctions for the time-independent Schrödinger equation from numerical solutions to the time-dependent equation. This method was developed earlier for determining eigenvalues and eigenfunctions of optical waveguide modes.² In the application of the method the solution $\psi(\mathbf{r}, t)$, which can be generated with the help of the split operator FFT method,³ is used to compute the correlation function $\phi_1(t) = \langle \psi(\mathbf{r}, 0) | \psi(\mathbf{r}, t) \rangle$. The numerical Fourier transform of $\phi_1(t)$, or $\phi_1(E)$, displays a set of sharp local maxima for $E = E_n$, where E_n are the desired energy eigenvalues. With the aid of line-shape fitting techniques, both the positions and heights of these resonances can be determined with high accuracy. The former yield the eigenvalues and the latter the weights of the stationary states that compose the wave packet. Once the eigenvalues are known, the corresponding eigenfunctions can be computed by numerically evaluating the integrals⁴

$$\psi(\mathbf{r}, E_n) = \int_0^T \psi(\mathbf{r}, t) w(t) \exp(iE_n t) dt, \quad (1)$$

where T is the time encompassed by the calculation, and $w(t)$ is a window function. For obvious reasons, we have called this method the spectral method.

In Ref. 1 it was demonstrated that the spectral method in conjunction with the split operator FFT solution of the time-dependent Schrödinger equation gives accuracy comparable with that of the variational method for the nontrivial two-dimensional Henon-Heiles potential. In this paper we describe some results obtained by applying the spectral method to a three dimensional Schrödinger equation with some standard Born-Oppenheimer potentials for nonlinear triatomic molecules: the Kuchitsu-Morino⁵ (KM) potential for SO_2 , the Barbe, Secroun, and Jouve⁶ (BSJ) potential for O_3 , and the Hoy,

Mills, and Strey⁷ (HMS) potential for H_2O . Vibrational levels have been determined with the variational method by Carney^{8,9} *et al.* for all three potentials and by Whitehead and Handy¹⁰ for the KM and HMS potentials. The semiclassical method has been applied to the KM and HMS potentials by Colwell and Handy¹¹ to determine a limited number of low-lying levels.

Results are also given for the spectral method applied to the independent normal mode approximation to the HMS potential used by Isaacson¹² *et al.* and obtained by expanding the potential in normal-mode coordinates and discarding cross terms. The energy eigenvalues for the resulting potential can then be computed from a set of 1-D calculations.¹³ Comparison between such results and those of a 3-D spectral method calculation provides a good test of the accuracy of the latter.

The principal attraction of the spectral method is its applicability with comparable efficiency and accuracy to a wide range of potentials, expressible in analytic form or as a set of numerical data. Both the accuracy and efficiency of the variational method, in contrast, are highly sensitive to the choice of basis functions.

Most of the computer time required by the spectral method is used in advancing the time-dependent solution of the Schrödinger equation. The latter¹ can be shown to scale as $MN^k \ln N$, where k is the number of space dimensions, N^k is the number of grid points or, equivalently, the number N^k of plane wave basis states used in the calculation, and M is the number of timesteps, which is determined by the desired resolution of the energy levels. In principle M does not vary with the dimensionality of the problem, but in practice the energy levels of systems of higher dimensionality tend to be more closely spaced, and may require multiple runs to isolate and distinguish. The computation time for the variational method scales with the number of basis states as N^{k^2} , and if numerical integration is required to evaluate the matrix elements a significant portion of the total computing time may be involved in setting up the Hamiltonian matrix. While no general statement

^{a)}Work performed under the auspices of the U. S. Department of Energy by the Lawrence Livermore National Laboratory under contract No. W-7405-ENG-48.

can be made concerning the relative efficiencies of the spectral and variational methods, the above considerations lead to the conclusion that the relative advantages of the spectral method should improve with the dimensionality of the problem.

The results furnished in this paper support the conclusion that not only can the spectral method be applied to three-dimensional potentials of practical interest, but that it is also capable of generating results not now accessible to other methods.

II. POTENTIAL ENERGY FUNCTIONS

We shall be concerned with Born-Oppenheimer potential functions for triatomic molecules of the form

$$V = \sum_i \sum_j K_{ij} \Delta R_i \Delta R_j + \sum_i \sum_j \sum_k K_{ijk} \Delta R_i \Delta R_j \Delta R_k + \sum_i \sum_j \sum_k \sum_l K_{ijkl} \Delta R_i \Delta R_j \Delta R_k \Delta R_l, \quad (2)$$

where the ΔR 's are displacements of the bond lengths and bond angles from equilibrium. In particular,

$$\begin{aligned} \Delta R_i &= r_i - r_e, \quad i=1, 2, \\ \Delta R_3 &= \theta - \theta_e. \end{aligned} \quad (3)$$

Here r_e and θ_e are the equilibrium bond length and bond angles, respectively, with $r_e = 1.4308 \text{ \AA}$ and $\theta_e = 119.32^\circ$ for SO_2 , $r_e = 1.2717 \text{ \AA}$ and $\theta_e = 116.8^\circ$ for O_3 , and $r_e = 0.9572 \text{ \AA}$ and $\theta_e = 104.52^\circ$ for H_2O . The values of the coefficients in Eq. (2) are listed for the three molecules in Table I.

III. HAMILTONIAN AND SCHRÖDINGER EQUATION FOR VIBRATIONAL MOTION

In order to utilize the potential energy function, it is necessary to introduce three sets of coordinates: the

Cartesians $\Delta x_i, \Delta y_i$ for each atom, the mass weighted Cartesians $q_1 = m_1^{1/2} \Delta x_1, q_2 = m_1^{1/2} \Delta y_1, \dots, q_5 = m_3^{1/2} \Delta x_3, q_6 = m_3^{1/2} \Delta y_3$, and the normal coordinates Q_1, \dots, Q_6 , which are derived from the potential in the usual way. The mass-weighted Cartesians and the normal coordinates are related through a unitary transformation, which enables the potential function (2) to be computed for a set of values of Q_1, \dots, Q_6 .

It is customary to express the Hamiltonian for a polyatomic molecule in a moving rotating frame of reference. The frame of reference moves in such a way that there can be no translation of the center of mass during a molecular vibration, and the rotation is chosen such that to zeroth order there can be no angular momentum within the frame of reference. This gives rise to a Hamiltonian, which has been derived in turn by Wilson and Howard,¹⁴ Darling and Dennison,¹⁵ and Watson.¹⁶

We shall assume for purely vibrational motion the following Schrödinger equation

$$i\hbar \frac{\partial \psi}{\partial t} = - \sum_{i=1}^3 \frac{\partial^2 \psi}{\partial Q_i^2} + V(Q_1, Q_2, Q_3) \psi, \quad (4)$$

where Q_1, Q_2 , and Q_3 are normal coordinates associated with the vibrational modes, Q_4 and Q_5 are normal coordinates associated with translation of the center of mass, Q_6 is the coordinate of the normal mode associated with a rotation of the three atoms in a plane, and $V(Q_1, Q_2, Q_3)$ is an abbreviation for $V(Q_1, Q_2, Q_3, Q_4=0, Q_5=0, Q_6=0)$. Omitted from Eq. (4) is a vibrational angular momentum term, which arises from the Coriolis interaction of two normal vibrations.¹⁴⁻¹⁶ As it turns out, this omission leaves us with an excellent approximation in the case of SO_2 and O_3 , but only a fair approximation in the case of H_2O .

IV. REVIEW OF THE SPECTRAL METHOD

For convenience we write the Schrödinger equation in terms of Cartesian coordinates in dimensionless form:

$$i \frac{\partial \psi}{\partial t} = - \frac{1}{2M} \nabla^2 \psi + V(x, y, z) \psi, \quad (5)$$

where

$$\nabla^2 = \frac{\partial^2}{\partial x^2} + \frac{\partial^2}{\partial y^2} + \frac{\partial^2}{\partial z^2}. \quad (6)$$

The symmetrically split operator algorithm³ for advancing the solution to Eq. (5) an incremental time Δt can be expressed formally as

$$\begin{aligned} \psi(x, y, z, t_0 + \Delta t) &= \exp \left(\frac{i\Delta t}{4M} \nabla^2 \right) \exp(-i\Delta t V) \exp \left(\frac{i\Delta t}{4M} \nabla^2 \right) \\ &\quad \times \psi(x, y, z, t_0) + O[(\Delta t)^3], \end{aligned} \quad (7)$$

where commutation errors give rise to the third order term in Δt , and the operator

$$\exp \left(\frac{i\Delta t}{4M} \nabla^2 \right), \quad (8)$$

applied to $\psi(x, y, z, t_0)$ is equivalent to solving the free particle wave equation

TABLE I. Internal force constants for potential in Eq. (2), where V is expressed in units of 10^{-12} erg, Δr in \AA and $\Delta \theta$ in radians.

	SO_2^a	O_3^b	H_2O^c
K_{11}	51.658	30.815	42.270
K_{33}	8.341	10.512	3.485
K_{12}	0.810	16.020	-1.010
K_{13}	3.246	5.112	2.190
K_{111}	-118.450	-91.531	-98.941
K_{112}	-5.737	-13.2111	1.265
K_{113}	-6.804	-15.800	2.020
K_{123}	-7.560	-13.000	-4.020
K_{133}	-9.013	-19.584	-1.125
K_{333}	-4.094	-6.307	-1.461
K_{1111}	165.127	164.480	160.029
K_{3333}	-6.143	14.555	-0.029
K_{1112}	-10.730	116.867	-8.266
K_{1113}	0.0	0.0	0.0
K_{1122}	-1.446	161.388	-1.424
K_{1133}	7.006	-82.000	-3.525
K_{1123}	0.0	0.0	0.0
K_{1233}	27.993	-158.000	3.050

^aReference 5.

^cReference 7.

^bReference 6.

$$i \frac{\partial \psi}{\partial t} = -\frac{1}{2M} \left(\frac{\partial^2 \psi}{\partial x^2} + \frac{\partial^2 \psi}{\partial y^2} + \frac{\partial^2 \psi}{\partial z^2} \right), \quad (9)$$

over a time $\Delta t/2$ with $\psi(x, y, z, t_0)$ as the initial wave function at $t = t_0$. The solution to Eq. (9) is obtained with the help of the band-limited Fourier series representation

$$\psi(x, y, z, t) = \sum_{l=-N/2+1}^{N/2} \sum_{m=-N/2+1}^{N/2} \sum_{n=-N/2+1}^{N/2} \psi_{lmn}(t) \times \exp 2\pi i \left[\frac{lx}{L_1} + \frac{my}{L_2} + \frac{nz}{L_3} \right], \quad (10)$$

where

$$\psi_{lmn}(t_0 + \Delta t) = \psi_{lmn}(t_0) \times \exp \left\{ -\frac{i\Delta t}{2M} (2\pi)^2 \left[\left(\frac{l}{L_1} \right)^2 + \left(\frac{m}{L_2} \right)^2 + \left(\frac{n}{L_3} \right)^2 \right] \right\}, \quad (11)$$

and L_1 , L_2 , and L_3 represent the lengths of the computational grid along directions parallel to the coordinate axes. The right-hand side of expression (7) is thus equivalent to free particle propagation over a half-time increment a phase change from the action of the potential applied over the whole time increment, and an additional free particle propagation over a half time increment.

The time increment Δt must be chosen small enough to assure accurate computation of the time-dependent wave function. The overriding criterion for this selection is based on the width of the energy spectrum, determined by the Fourier transform of $\langle \psi(x, y, z, 0) \times \psi(x, y, z, t) \rangle$. The sampling interval Δt should be chosen small enough to accommodate at least the entire spectrum of bound state energy levels, or

$$\Delta t \ll \pi / \Delta V_{\max}, \quad (12)$$

where ΔV_{\max} is the maximum excursion of the potential. If the potential under consideration is unbounded, it will be necessary to apply an appropriate bound in order to apply the method.

The excitation of energy eigenstates is controlled by the choice of the initial wave function $\psi(x, y, z, 0)$. Usually this selection is governed by symmetry considerations, since it may be desired to either generate or suppress classes of states belonging to particular symmetries. This selective excitation of states can be used, for example, to avoid the simultaneous presence of nearly degenerate states whose energy eigenvalues could be difficult to resolve in the computed energy spectrum.

The solution to Eq. (2) can be expressed as a linear superposition of eigenfunctions,

$$\psi(x, y, z, t) = \sum_{n,j} A_{nj} u_{nj}(x, y, z) \exp(-iE_n t), \quad (13)$$

where the index j is used to distinguish states within a degenerate set and $u_{nj}(x, y, z)$ satisfies

$$-(1/2M) \nabla^2 u_{nj} + V(x, y, z) u_{nj} = E_n u_{nj}. \quad (14)$$

Let us define the correlation function $\mathcal{P}_1(t)$ as

$$\mathcal{P}_1(t) = \langle \psi(x, y, z, t, 0) | \psi(x, y, z, t) \rangle$$

$$= \int \int \psi^*(x, y, z, 0) \psi(x, y, z, t) dx dy dz. \quad (15)$$

Using expression (13) in Eq. (15) gives

$$\mathcal{P}_1(t) = \sum_{n,j} |A_{nj}|^2 \exp(-iE_n t). \quad (16)$$

If we now multiply the right-hand side of Eq. (16) by the normalized Hanning window function $w(t)/T$, where

$$w(t) = \begin{cases} 1 - \cos \frac{2\pi t}{T}, & 0 \leq t \leq T \\ 0, & t \geq T, \end{cases} \quad (17)$$

and Fourier transform with respect to t , the result is

$$\mathcal{P}_1(E) = \sum_n W_n \mathcal{L}_1(E - E_n), \quad (18)$$

where the relative weights of the states are

$$W_n = \sum_j |A_{nj}|^2, \quad (19)$$

and the line-shape function $\mathcal{L}_1(E - E_n)$ is defined by

$$\begin{aligned} \mathcal{L}_1(E - E_n) &= \frac{1}{T} \int_0^T \exp[i(E - E_n)t] w(t) dt \\ &= \frac{\exp[i(E - E_n)T] - 1}{i(E - E_n)T} - 1/2 \left[\frac{\exp[i((E - E_n)T + 2\pi)] - 1}{i[(E - E_n)T + 2\pi]} \right. \\ &\quad \left. + \frac{\exp[i((E - E_n)T - 2\pi)] - 1}{i[(E - E_n)T - 2\pi]} \right]. \end{aligned} \quad (20)$$

The correlation function $\mathcal{P}_1(t)$ is evaluated numerically by trapezoidal integration for each timestep, the Fourier transform $\mathcal{P}_1(E)$ is evaluated numerically from the sampled values of $\mathcal{P}_1(t)$ upon completion of the desired number of integration steps, and, finally, the data set for $\mathcal{P}_1(E)$ is fit to the form Eq. (18). For most cases excellent results are obtained by assuming a single-line fit or¹⁷

$$\mathcal{P}_1(E) = W_n \mathcal{L}_1(E - E_n). \quad (21)$$

If both sides of Eq. (13) are multiplied by $T^{-1} w(t) \exp(iEt)$ and integrated from 0 to T , the result is

$$\begin{aligned} \psi(x, y, z, E) &= \frac{1}{T} \int_0^T \psi(x, y, z, t) w(t) \exp(iEt) dt \\ &= \sum_{n,j} A_{nj} u_{nj}(x, y, z) \mathcal{L}_1(E - E_n). \end{aligned} \quad (22)$$

The function $\psi(x, y, z, E)$ will exhibit a maximum whenever $E = E_n$. For negligible overlap between the resonant terms in Eq. (22), one obtains to an excellent approximation

$$\psi(x, y, z, E_n) = \sum_j A_{nj} u_{nj}(x, y, z) \mathcal{L}_1(0). \quad (23)$$

If one chooses the initial wave function $\psi(x, y, z, 0)$ so that at most one member of a degenerate set of states is excited at one time, the numerical computation of a particular eigenfunction $u_n(x, y, z)$ reduces to the numerical integration

$$\begin{aligned} u_n(x, y, z) &= \text{const} \int_0^T \psi(x, y, z, t) w(t) \exp(iE_n t) dt \\ &= \text{const} \psi(x, y, z, E_n). \end{aligned} \quad (24)$$

V. NUMERICAL RESULTS

All computations were performed with 16 384 time steps on a $32 \times 32 \times 32$ grid. Grid spacings and sizes were chosen to be different in all three principal directions, based on several considerations. First, the grid spacings need to be small enough to resolve the ground state wave function, and second, the grid should be large enough to accommodate the wave functions of all states of interest. Once the grid dimensions have been chosen, an effective cutoff of the potential is determined. That cutoff represents an upper bound to the energy eigenvalues that can be determined from the calculation. Accurate eigenvalues and corresponding wave functions can be expected for energy levels up to about 80% of the cutoff energy. (Wave functions for states too close to the cutoff may be insufficiently attenuated at the grid boundary and consequently could undergo an unphysical reflection.) Table II contains the normal frequencies, cutoff values of the potentials, and the grid parameters used in computations for the three molecules.

When the computed spectrum $\rho(E)$ is scanned, it is possible for two or more eigenstates to be identified as one, if the corresponding eigenvalues are so close that their resonant peaks cannot be resolved. This may lead to a problem in identifying all of the states, particularly as the states cluster closer together with higher energy. It is therefore desirable to thin out the states by initially exciting only states of specific symmetry. For each of the three molecules one run was made in which it was attempted to excite as many as possible of the states below cutoff. This was done by employing an initial wave function of the form

$$\psi(Q_1, Q_2, Q_3, 0) = \prod_{i=1}^3 w(Q_i) \exp(-Q_i^2/2\sigma_i^2) \sum_{n=1}^4 (Q_i/\sigma_i)^n, \quad (25)$$

where the σ_i are chosen a little larger than the radius of the ground state wave function for a simple harmonic oscillator of the appropriate normal frequency, and $w(Q_i)$ are Hanning window functions appropriate to the grid. The function (25) was intended to contain contributions of all possible parities in Q_1 , Q_2 , and Q_3 , but its selection was otherwise quite arbitrary. Only for

TABLE II. Normal frequencies (cm^{-1}), potential cutoffs V_{max} (cm^{-1}) due to finite grid size, and increments ΔQ_i and lengths L_i of the 3-D normal coordinate grid (\AA).

	SO ₂	O ₃	H ₂ O
ω_1	1171	1135	3832
ω_2	525	716	1649
ω_3	1378	1089	3942
V_{max}	10 000	10 000	18 000
ΔQ_1	0.053	0.094	0.030
ΔQ_2	0.094	0.100	0.053
ΔQ_3	0.030	0.063	0.030
L_1	1.7	3.0	0.95
L_2	3.0	3.2	1.7
L_3	1.6	2.0	0.95

normal coordinate Q_3 , the bending mode coordinate, however, does the potential and consequently the wave function have a true parity. Second and third runs were subsequently made in which only states of even and odd parity, respectively, in Q_3 were excited. This was done using the initial wave functions

$$\psi_e(Q_1, Q_2, Q_3, 0) = w(Q_3) \exp(-Q_3^2/2\sigma_3^2) \times \prod_{i=1}^2 w(Q_i) \exp(-Q_i^2/2\sigma_i^2) \sum_{n=1}^4 (Q_i/\sigma_i)^n, \quad (26a)$$

$$\psi_o(Q_1, Q_2, Q_3, 0) = w(Q_3) Q_3^3 \exp(-Q_3^2/2\sigma_3^2) \times \prod_{i=1}^2 w(Q_i) \exp(-Q_i^2/2\sigma_i^2) \sum_{n=1}^4 (Q_i/\sigma_i)^n. \quad (26b)$$

For each of the molecules all of the lowest ten or so energy-levels could be identified in the single all-parity run. As would be expected, additional levels were discovered in the pair of runs involving but a single parity with respect to Q_3 . As would also be expected, the incidence of such additional levels increased with energy.

Computations were performed on a CRAY I computer with runs taking about 15 min each. This time may not be considered excessive, when it is borne in mind that each computation encompassed 32 768 grid points and 16 384 time steps and could generate about 50 energy eigenvalues. The efficiency of the calculation derives not only from the inherent efficiency of the FFT al-

TABLE III. Twenty lowest vibrational energy levels (in cm^{-1}) of SO₂ for KM potential, including vibrational quantum numbers. Results are given for simple harmonic oscillator approximation (SHO), perturbation theory (PT), semi-classical method (SC), variational method (VM), and spectral method (SM).

	SHO	PT ^a	SC ^b	VM ^c	SM ^d
$v_1 v_2 v_3$	1537	1529	1529	1530	1530
0 1 0	2062	2045	2045	2047	2046
0 2 0	2586	2556	2556	2557	2556
1 0 0	2708	2684	2685	2686	2686
0 0 1	2915	2888	2889	2890	2890
0 3 0	3110	3062	3060	...	3060
1 1 0	3233	3198	3119	3201	3200
0 1 1	3439	3400	3401	3403	3401
0 4 0	3636	3562	3558	...	3557
1 2 0	3757	3707	3707	...	3708
2 0 0	3879	3831	3833	3835	3835
0 2 1	3964	3907	3908	...	3907
1 0 1	4086	4029	4034	4035	4035
0 5 0	4160	4056	4049	...	4048
1 3 0	4282	4209
0 0 2	4292	4236	...	4241	4241
2 1 0	4404	4344	4347
0 3 1	4488	4406
1 1 1	4610	4540	4544
0 6 0	4685	4545	4531

^aReference 12.

^bReference 11.

^cReference 8.

^dPresent work.

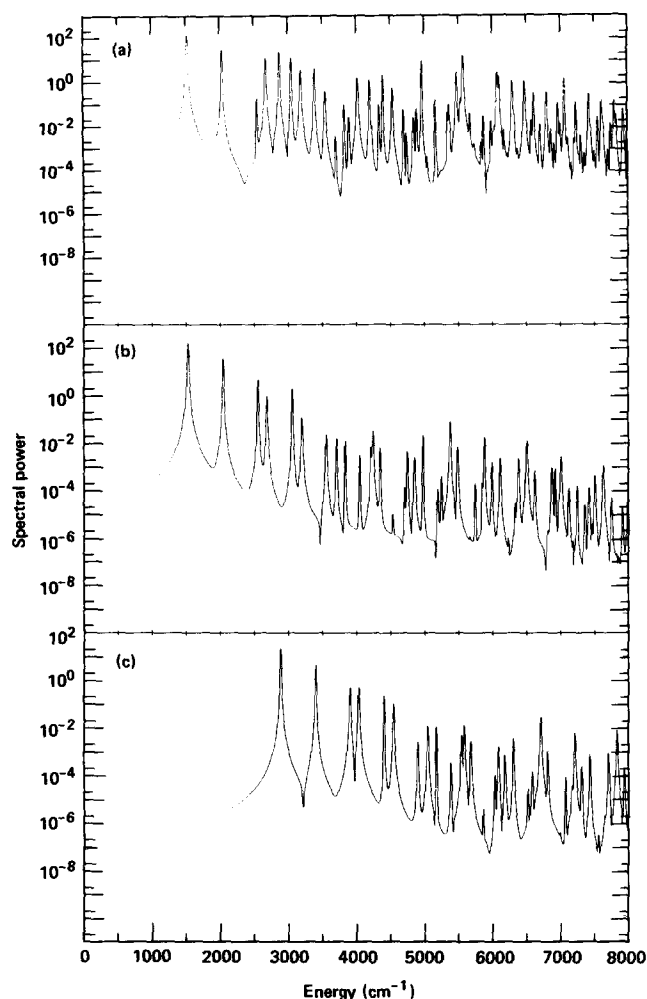


FIG. 1. Energy spectra for vibrational levels of SO_2 computed from the Kuchitsu-Morino potential: (a) all parity states excited, (b) even parity states in Q_3 (bending mode) excited, (c) odd parity states in Q_3 excited.

gorithm, but also from the extensive vectorization of the 3-D FFT computations. The adequacy of the $32 \times 32 \times 32$ spatial grid for the range of vibrational levels generated in these runs attests to the high spatial accuracy of the split operator FFT method applied to the time-dependent Schrödinger equation.¹⁻³

A. SO_2

The 20 lowest energy eigenvalues for SO_2 calculated with the spectral method (SM) and the KM potential⁵ are given in Table III. Also included for comparison are results from the simple harmonic oscillator approximation (SHO), perturbation theory¹² (PT), the semi-classical method¹⁰ (SC), and the variational method⁸ (VM). The quantum numbers refer to the lowest energy state represented in either the perturbation expansion or the variational function, where available. Spectral method and variational method results where available are in excellent agreement. Where they differ the spectral method results tend to be 1–2 cm^{-1} lower than the variational method results. However, this does not necessarily imply greater accuracy for the former,

since the spectral method is not based on the Watson Hamiltonian,¹⁸ whereas the variational results are. With the exception of level (110), the available semi-classical values are also in good agreement with the spectral method results.

Eighty-four additional energy levels determined by the spectral method are listed in Table IV. No attempt has been made to classify them other than by parity in Q_3 , nor can it be guaranteed that they are the only eigenvalues within the energy interval they span. They should, in any case, be accurate to 1 or 2 cm^{-1} . The complete set of eigenvalues is displayed in Fig. 1, which contains the energy spectra for all three runs. Representative eigenfunctions computed with the help of Eq. (24) are displayed in Figs. 2 and 3, where contours of the corresponding probability density functions $|\psi(x, y, z)|^2$ are plotted on coordinate planes.

The spectral method was also applied to the harmonic potential appropriate to SO_2 with the same grid. Representative eigenvalues obtained from this calculation are listed in Table V and compared with their analytic counterparts. The two sets of eigenvalues agree to within 1 cm^{-1} overall and differ by $\sim 2 \text{ cm}^{-1}$ only for the highest level listed. This comparison provides an estimate of the accuracy for the energy levels determined for the KM potential.

TABLE IV. Additional energy levels (in cm^{-1}) for SO_2 computed by the spectral method for the KM potential. Levels are arranged in order of increasing energy and according to parity in Q_3 .

odd	even	odd	even	odd	even
	4705		6330		7630
	4748		6380	7640	
	4853		6475	7706	
4899			6486		7749
	4977		6505	7803	
	5019	6519			7911
5047		6583		7937	
5173			6620		7997
	5193	6670		8035	
	5249	6711			8040
	5352	6799		8124	
	5376	6811			8132
5385			6873	8195	
	5487		6920		8249
5544			6980	8250	
5584		6996		8292	
	5673		7009		8310
5680		7074		8332	
	5744		7122		8376
	5845	7167		8434	
5863		7212			8481
	5881		7243	8502	
	5990		7285		8537
6035		7310		8559	
6087			7359		8586
	6112		7418		
6182		7433			
	6233		7459		
6305			7506		
		7559			

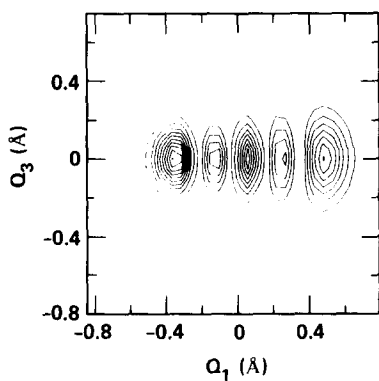
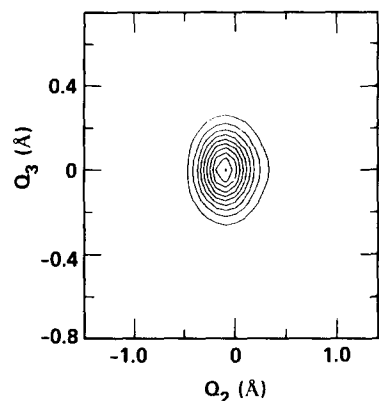
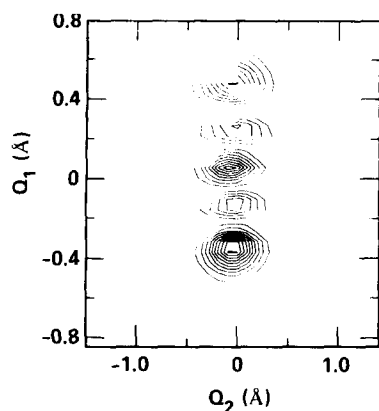


FIG. 2. Probability density contours from energy eigenfunctions for SO_2 corresponding to vibrational level $E = 6112 \text{ cm}^{-1}$.

TABLE V. Selected harmonic oscillator energy levels (cm^{-1}) computed analytically (SHO) from normal frequencies $\omega_1, \omega_2, \omega_3$ and numerically with the spectral method (SM), using harmonic potential for SO_2 .

	SHO	SM
$v_1 v_2 v_3$		
0 0 0	1536.8	1537.0
0 1 0	2061.5	2061.7
0 2 0	2586.2	2586.4
1 0 0	2707.9	2708.2
0 0 1	2914.6	2915.0
0 3 0	3110.9	3111.1
1 1 0	3232.6	3232.9
0 1 1	3439.3	3439.7
0 4 0	3635.6	3635.9
1 2 0	3757.3	3757.6
2 0 0	3879.0	3879.4
0 2 1	3964.0	3964.4
1 0 1	4085.7	4086.2
0 5 0	4160.4	4160.6
0 0 2	4292.4	4293.2
2 1 0	4403.7	4404.1
0 3 1	4488.7	4489.1
1 1 1	4610.4	4610.9
0 6 0	4685.1	4685.3
3 0 0	5050.0	5050.6
0 5 1	5538.1	5538.7
1 1 2	5988.2	5989.9
2 2 1	6306.2	6306.9
0 5 2	6916.0	6916.6
3 2 1	7477.3	7478.7
2 2 2	7684.0	7685.4
5 1 0	7916.9	7917.9
3 1 2	8330.3	8331.7
3 2 2	8855.1	8857.1

B. O_3

The 14 lowest energy levels for the BSJ potential⁶ for O_3 computed with the spectral method are listed in Table VI along with the corresponding variational method

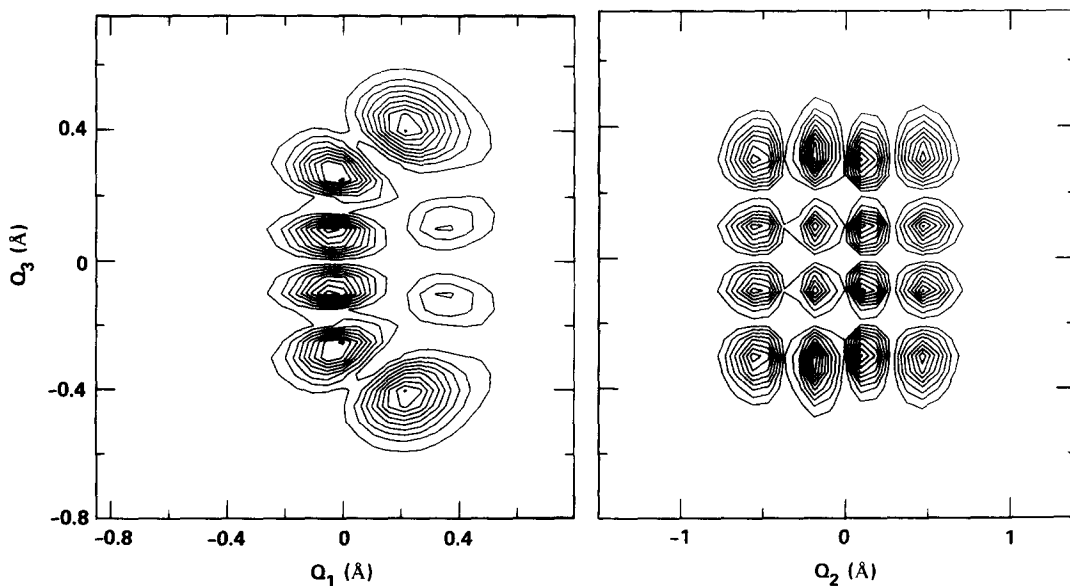


FIG. 3. Probability density contours for SO_2 energy eigenfunction with $E = 8195 \text{ cm}^{-1}$. The eigenfunction vanishes for $Q_3 = 0$, hence there is no plot over Q_1 - Q_2 plane.

TABLE VI. Computed vibrational energy levels (in cm^{-1}) of O_3 for BSJ potential. Variational method (VM) and spectral method (SM) compared.

	VM ^a	SM ^b
$v_1 v_2 v_3$		
0 0 0	1457	1457
0 1 0	2157	2157
0 0 1	2504	2504
1 0 0	2564	2565
0 2 0	2853	2852
0 1 1	3185	3184
1 1 0	3254	3253
0 0 2	3535	3534
0 3 0	3542	3541
1 0 1	3588	3587
2 0 0	3670	3669
0 2 1	3860	3859
1 2 0	3943	3942
0 1 2	4198	4195

^aReference 9.^bPresent work.

results from Ref. 9. Again the agreement is seen to be very good.

C. H_2O

The 14 lowest energy levels computed with the spectral method are compared with corresponding values determined with the variational method⁹ in Table VII. The agreement is notably poorer than that encountered for the SO_2 and O_3 potentials. This poorer agreement is attributed to the importance of the Coriolis terms in the Watson¹⁶ Hamiltonian for H_2O , which was the basis of the computations in Ref. 8. To check the numerical accuracy of the spectral method as applied to the HMS potential, a fully three-dimensional computation was performed using the corresponding independent normal

TABLE VII. Computed vibrational energy levels (in cm^{-1}) for H_2O for HMS potential. Comparison between variational method (VM) and spectral method (SM).

	VM ^a	SM ^b
$v_1 v_2 v_3$		
0 0 0	4 653	4 663
0 1 0	6 249	6 248
0 2 0	7 811	7 797
1 0 0	8 369	8 381
0 0 1	8 473	8 471
0 3 0	9 336	9 308
1 1 0	9 952	9 951
0 1 1	10 055	10 015
0 4 0	10 828	10 779
1 2 0	11 498	11 483
0 2 1	11 602	11 523
2 0 0	12 072	12 083
1 0 1	12 173	12 171

^aReference 9.^bPresent work.TABLE VIII. Computed energy levels for H_2O for independent normal mode potential derived from HMS potential.

	INM ^a	INMSM ^b
$v_1 v_2 v_3$		
0 0 0	4 728	4 728
0 1 0	6 366	6 366
0 2 0	7 995	7 995
1 0 0	8 490	8 491
0 0 1	8 772	8 773
0 3 0	9 616	9 615
1 1 0	10 128	10 129
0 1 1	10 410	10 410
0 4 0	11 230	11 229
1 2 0	11 758	11 757
0 2 1	12 039	12 039
2 0 0	12 204	12 205
1 0 1	12 534	12 535
0 0 2	12 911	12 913

^aReference 12.^bPresent work.

mode potential in Eq. (4). The independent normal mode potential can be expressed as $V_{\text{INM}}(Q_1, Q_2, Q_3) = V_1(Q_1) + V_2(Q_2) + V_3(Q_3)$, where $V_1(Q_1) = V(Q_1, 0, 0)$, $V_2(Q_2) = V(0, Q_2, 0)$, $V_3(Q_3) = V(0, 0, Q_3)$, and $V(Q_1, Q_2, Q_3)$ is the potential (2) expressed in terms of normal coordinates. The results of this computation are compared with corresponding results from Ref. 12, obtained from one-dimensional computations. The agreement is seen to be very good, supporting the conclusion that the spectral method gives accurate eigenvalues for the HMS potential.

VI. SUMMARY AND CONCLUSIONS

We have shown that the spectral method, applied previously to two-dimensional potentials, can be used to determine accurate eigensolutions for some practical three-dimensional Born-Oppenheimer potentials. In particular, we have demonstrated very good agreement between the spectral and variational methods for low lying vibrational energy levels of SO_2 and O_3 . The same computation also yielded numerous higher lying energy levels for SO_2 not available from the variational method. The accuracy of these energy levels was established by computing energy levels for the corresponding harmonic potential.

The spectral method was also applied to the HMS potential for H_2O , but here the absence of Coriolis terms in the Hamiltonian led to poorer agreement with variational method results. Despite this poorer agreement, the accuracy of the spectral method computation for the HMS potential was established by computing the eigenvalues for the corresponding independent normal mode potential and comparing them with values based on one-dimensional computations.

¹M. D. Feit, J. A. Fleck, Jr., and A. Steiger, J. Comp. Phys. (to be published).

²M. D. Feit and J. A. Fleck, Jr. Appl. Opt. **19**, 2240 (1980);

- J. Opt. Soc. Am. **17**, 1361 (1981).
- ³J. A. Fleck, Jr., J. R. Morris, and M. D. Feit, Appl. Phys. **10**, 129 (1976).
- ⁴In this respect our method resembles the method devised by Davis and Heller, who utilize a semiclassical form of $\psi(\mathbf{r}, t)$ to derive the eigenfunction $\psi(\mathbf{r}, E_n)$. See M. J. Davis and E. J. Heller, J. Chem. Phys. **75**, 3916 (1981).
- ⁵K. Kuchitsu and Y. Morino, J. Chem. Soc. Jpn. **38**, 814 (1965).
- ⁶A. Barbe, C. Secroun, and P. Jouve, J. Mol. Spectrosc. **49**, 171 (1974).
- ⁷A. R. Hoy, I. M. Mills, and G. Strey, Mol. Phys. **24**, 1265 (1972).
- ⁸G. D. Carney and C. W. Kern, Int. J. Quantum Chem. Symp. **9**, 317 (1975).
- ⁹G. D. Carney, L. A. Curtiss, and S. R. Langhoff, J. Mol. Spectrosc. **61**, 371 (1976).
- ¹⁰R. J. Whitehead and N. C. Handy, J. Mol. Spectrosc. **55**, 356 (1975).
- ¹¹S. M. Colwell and N. C. Handy, Mol. Phys. **35**, 1183 (1978).
- ¹²A. D. Isaacson, D. G. Truhlar, K. Scanlon, and J. Overend, J. Chem. Phys. **75**, 3017 (1981).
- ¹³D. G. Truhlar, J. Comp. Phys. **10**, 123 (1972).
- ¹⁴E. B. Wilson and J. B. Howard, J. Chem. Phys. **4**, 260 (1936).
- ¹⁵D. M. Dennison and B. T. Darling, Phys. Rev. **57**, 128 (1940).
- ¹⁶J. K. G. Watson, Mol. Phys. **15**, 479 (1968).
- ¹⁷The details of this fit can be found in Ref. 1.